# Single Cell Mechanics: Stress Stiffening and Kinematic Hardening

Pablo Fernández* and Albrecht Ott†

*Experimentalphysik I, Physikalisches Institut, Universität Bayreuth, D-95440 Bayreuth, Germany*

(Received 27 June 2007; published 13 June 2008)

Cell mechanical properties are fundamental to the organism but remain poorly understood. We report a comprehensive phenomenological framework for the complex rheology of single fibroblast cells: a superposition of elastic stiffening and viscoplastic kinematic hardening. Despite the complexity of the living cell, its mechanical properties can be cast into simple, well-defined rules. Our results reveal the key role of crosslink slippage in determining mechanical cell strength and robustness.

DOI: 10.1103/PhysRevLett.100.238102 PACS numbers: 87.15.La, 83.60.Df, 83.60.La, 87.16.Ka

Intracellular transport, cell locomotion, resistance to external mechanical stress and other vital biomechanical functions of eukaryotic cells are governed by an active biopolymer gel: the cytoskeleton [1]. This gel is made up of three types of biopolymers: actin, microtubules, and intermediate filaments. These are crosslinked by a multitude of associated proteins with different properties in terms of connection angles, bond strengths, and bond lifetimes. The actin cytoskeleton—the major force-sustaining structure in the cell—is made up of filaments with lengths of the order of a micrometer and presents a weak, local structural order. The cytoskeleton also comprises molecular motors, associated proteins which move along actin or microtubule filaments driven by chemical energy. It is not understood how the cytoskeleton, in conjunction with biochemical regulatory circuits, performs specific active mechanical tasks. When cells attach to biological material they often biochemically recognize the binding partner. The cytoskeleton organizes accordingly and produces a mechanical response. Active cell responses such as contraction are well separated from passive rheological properties by the time scales over which they occur [2]. Passive cell rheological properties have been studied with various techniques on the subcellular and supercellular scale [3]. Through various measurement techniques on different eukaryotic cell types, a broad relaxation spectrum has arisen as a common feature of passive, linear cell rheology [3,4]. The description of the nonlinear regime remains elusive; both stress stiffening [5–9] and linear responses to large stretch [8–11] have been observed.

In this Letter we present experiments in which individual cells are stretched between two plates using a microplate rheometer [2,7] (Fig. 1). In earlier work, we have shown that small, quasidifferential cell deformations reveal an essentially elastic response described by a differential modulus that is dependent on cell prestress but independent of cell length [7]. Here we show that large deformations reveal an inelastic response with a (counterintuitive) linear force-length relation, and that both regimes superpose to generate the response to more complex deformations. When the inelastic cell response is abolished by biochemical fixation (which maintains the structure but prevents crosslink sliding) the cell exhibits the nonlinear response which can be predicted from the measurement of the differential modulus. Thus, despite the complexity of the eukaryotic cell cytoskeleton and immense cell heterogeneity, passive nonlinear cell rheology can be reduced to simple rules.

*Experimental setup.*—We refer to [2,7] for details. A 3T3 fibroblast [12] adheres between two fibronectin-coated glass microplates. One of them is flexible: its deflection gives the force $F$ acting on the cell in the direction perpendicular to the plate surface. A computer reads $F$ and the cell length $L$, and adjusts the position of the plate using a piezoelectric actuator as a function of the given experimental protocol. Experiments are performed at 35 °C, in standard medium with Lysophosphatidic acid 50 $\mu$M (Sigma). All results described here are reproducible for strongly adhering fibroblasts that sustain pulling forces of 100 nN for several hours; this ends up being about 30% of the cells in culture.

*Loading and unloading at constant rate.*—We stretch the cell by 100% at a constant-rate $\dot{L}$ while measuring the force $F$ [Fig. 2(a)]. The initial slope $dF/dL$ decreases until reaching a constant value at a stretch ~10% [Fig. 2(b)].

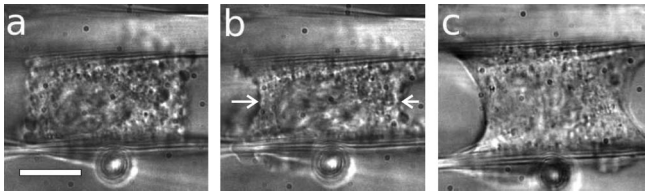


FIG. 1. A fibroblast adhering between two microplates. The cell has a well-controlled and simple geometry. It adheres to the microplates via biochemical linkers, which help define the state of the cell cytoskeleton. (a) Right after contact. Bar: 10 $\mu$m. (b) After ~20 min at 35 °C, strongly adhering cells often adopt a concave shape. From the apparent diameter $D_0$ (arrows) we estimate the initial area $A_0 := \pi(D_0/2)^2$. (c) Under large stretch.

 

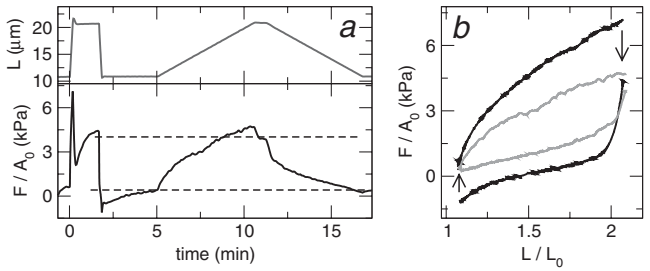


FIG. 2. Loading and unloading at constant rate $\dot{L}$. (a) Imposed length $L$ and measured Lagrangian stress $F/A_0$ (where $A_0$ is the initial cell contact area) as a function of time. After each ramp, $F$ stabilizes at a nonzero value $\mathfrak{F}$ (dotted line). (b) $F/A_0$ as a function of $L/L_0$ (where $L_0$ is the steady zero-force-length) during loading and unloading. Black curve: $\dot{L} = 1\ \mu$m/s. Gray curve: $\dot{L} = 0.03\ \mu$m/s.

Beyond 10% and up to 100% stretch, the $F(L)$ relation is approximately linear. After loading, the cell length $L$ is held constant for a few minutes; the force $F$ relaxes to a steady nonzero value $\mathfrak{F}$ which does not evolve faster than about 1 nN/s. An analogous response is observed upon unloading. The procedure is repeated with different rates $\dot{L}$ between 3 nm/s and 10 $\mu$m/s. The rest force $\mathfrak{F}$ is independent of the loading rate in the explored range.

*Small amplitude stiffening, large amplitude linearity.*—To explore small and large deformation amplitudes simultaneously, we perform a ramping perturbation with superimposed harmonic oscillations, $L(t) = vt + \Delta_L \sin(\omega t)$. Figure 3 shows a typical experiment. The response to small oscillations indeed stiffens with increasing stress. Yet, the average over an oscillation period of the force $\langle F \rangle$ and length $\langle L \rangle$ are linearly related as inferred from the position of the loops. Thus, we observe both responses as a superposition: stress stiffening for small amplitude deformations

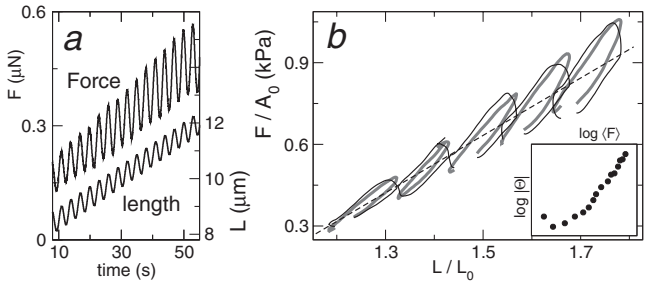


FIG. 3. Small amplitude stiffening, large amplitude linearity. (a) $F$ and $L$ as a function of time. (b) $F/A_0$ as a function of $L/L_0$. For clarity only a few loops are shown. Gray curves: experimental data. Black curves: fit using Eqs. (1)–(5), with $\gamma = 5$ and $\beta = 0.25$. The dashed line highlights the linear relation between the average values. Inset: "Differential" modulus $|\Theta|$ from the oscillations as a function of average force $\langle F \rangle$ for the data in (b). The modulus exhibits stress stiffening, following the master relation reported in [7].

(as reported in [7]) in addition to a linear force-length relation at large deformations.

*Small amplitude reversibility, large amplitude irreversibility.*—We study the amplitude dependence at a constant deformation rate $|\dot{L}|$. The essential feature of this protocol [Fig. 4(a)] are the turning points separated at various distances. This is done to study the reversibility of the response. As Fig. 4(b) shows, the reversibility of the response upon a change of direction is determined by the distance to the previous turning point. Where turning points are separated by less than 10% stretch, the response is reversible (elastic). More than 10% stretch beyond a turning point, the response becomes irreversible (inelastic): the $F(L)$ curve does not retrace its path upon direction reversal. In this inelastic regime the $F(L)$ relation is approximately linear. Its nonzero slope leads to a translation of the elastic region by the inelastic deformation, a behavior known in plasticity as linear kinematic (or directional) hardening [13,14]. The inelastic contraction under pulling tension between X and G in Fig. 4(b) is a strong Bauschinger effect (a decrease in yield stress upon unloading) [15].

*Rate dependence.*—In the inelastic regime the hysteresis becomes more pronounced with increasing stretch rate

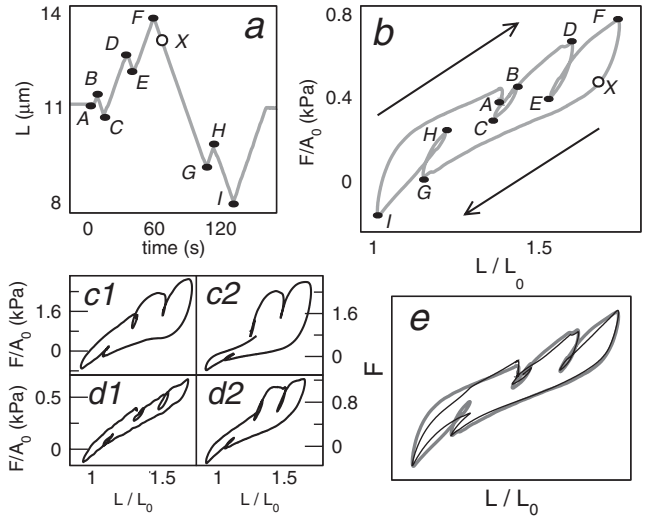


FIG. 4. Elastic/inelastic behavior. (a) Imposed length $L$ as a function of time. (b) $F/A_0$ as a function of $L/L_0$ for a given cell. Reversible (elastic) behavior upon direction reversal is observed only close to a previous turning point, as in C, E, H. The response becomes irreversible (inelastic) after a steady large deformation: at the turning points D, F, G, I, the $F(L)$ curve does not retrace its previous path. Between $F$ and $I$ the experiment is equivalent to C–F, but in the unloading direction. Since the response is equivalent, the sense of deformation is irrelevant. (c1) Another cell, probed at a rate $\dot{L} = 0.1\ \mu$m/s. (c2) Same cell as c1 but at $\dot{L} = 1\ \mu$m/s. (d1) Another cell, 0.1 $\mu$m/s. (d2) Same cell as d1, 1 $\mu$m/s. (e) Fit using Eqs. (1)–(5) (black curve) to the data shown in Fig. 4(b) (gray curve), with $\gamma = 8$ and $\beta = 0.24$.

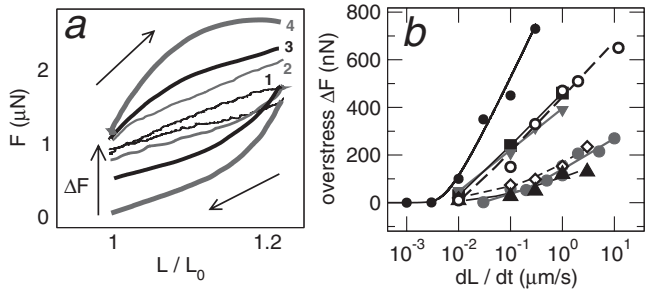


FIG. 5. Loading and unloading for several rates $\dot{L}$. (a) $F$ as a function of $L/L_0$ for a given cell, where $L_0$ is the initial length. Rates are: (1) 10 nm/s, 2) 30 nm/s, 3) 0.1 $\mu$m/s, 4) 1 $\mu$m/s. The overstress $\Delta F$ is defined as the extent of relaxation after unloading. (b) $\Delta F$ as a function of rate $\dot{L}$ for 7 different cells (symbols). The curves are fits to Eq. (3).

[Figs. 2(b) and 5(a)]. To characterize this rate-dependence, we define the overstress $\Delta F$ as the extent of force relaxation after unloading [Fig. 5(a)]. The overstress $\Delta F$ behaves as $\log(dL/dt)$ approaching zero at a stretching rate of about 10 nm/s [Fig. 5(b)]. The logarithmic trend does not hold for $\Delta F < 100$ nN. Characterization of this regime is difficult due to the onset of erratic, active cell behavior. From Figs. 4 and 5, we conclude: irreversibility requires both large stretch amplitudes and stretch rates above 10 nm/s; for reversibility, either small amplitudes (below 10% stretch) or rates around 10 nm/s suffice.

*Large amplitude stiffening after glutaraldehyde fixation.*—We add glutaraldehyde 0.1% in order to prevent slippage of cytoskeletal connections, a procedure named fixation. The increasing slope of the curve labeled fixed in Fig. 6(b) now reveals a stiffening response for continuing stretch. The numerical derivative of the $F(L)$ relation obtained from fixed (hence dead) cells is the same as the differential master-relation obtained from living fibroblasts [Fig. 6(c), from Ref. [7]). This $F(L)$ relation closely resembles the exponential stress-stretch relations observed in whole tissues [16,17].

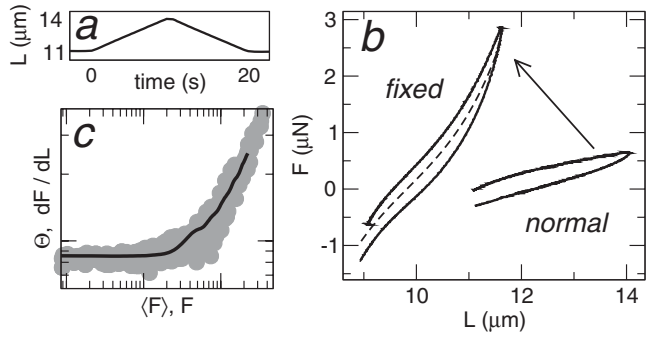


FIG. 6. (a) Controlled length $L$ as a function of time. A single loading cycle with amplitude 30% is performed. (b) Force $F$ as a function of length $L$. "Normal": before adding glutaraldehyde. "Fixed": in presence of glutaraldehyde 0.1%. The dotted line is a fit to Eq. (2). (c) The derivative $dF/dL$ of the fixed curve (black line) plotted against the differential master-relation (gray dots, as discussed in Ref. [7]).

*Viscoplasticity.*—We propose a minimal constitutive relation for fibroblasts under uniaxial extension. We decompose the measurable cell length $L$ into inelastic zero-force length $\mathfrak{L}$ and elastic stretch ratio,

$$L = \lambda\mathfrak{L}. \tag{1}$$

The force is a function of the elastic strain,

$$F \propto (\lambda - 1)e^{\gamma(\lambda^2+2/\lambda-3)}, \tag{2}$$

where we use exponential elasticity [16], according to Fig. 6(b) and 6(c). The flow rule relates the inelastic flow rate $\dot{\mathfrak{L}}$ to the overstress $F - \mathfrak{F}$. We obtain reasonable agreement with experiments [Fig. 5(b)] using

$$\dot{\mathfrak{L}} \propto \mathrm{sgn}(F - \mathfrak{F})(|F - \mathfrak{F}|/\mathcal{D})^{\beta}e^{|F-\mathfrak{F}|/\mathcal{D}}, \tag{3}$$

with $\beta \simeq 0.1 - 0.5$. The drag force $\mathcal{D}$ sets the scale where the overstress induces the transition from elastic to inelastic deformation [7]. The rest force $\mathfrak{F}$ accounts for kinematic hardening [13,14]:

$$\dot{\mathfrak{F}} \propto \dot{\mathfrak{L}}. \tag{4}$$

For constant-rate loading the deformation becomes inelastic, $\dot{\mathfrak{L}} \to \dot{L}$, as the overstress approaches a steady value $\Delta F \propto \mathcal{D}$. Hence the drag force $\mathcal{D}$ defines the force-width of the hysteresis of the inelastic response [Fig. 5(a)]. Since the hysteresis loop broadens at high forces with increasing $F$ [Fig. 2(b)], $\mathcal{D}$ must increase roughly linearly with $F$. That is, $\mathcal{D}$ behaves just like the differential elastic modulus [Fig. 3(b), inset]. We therefore suggest

$$\mathcal{D}(F) \propto dF/d\lambda, \tag{5}$$

which is equivalent to the relation between the loss and storage moduli of the small amplitude response [7]. As Figs. 3(b) and 4(e) show, the constitutive relation captures the essence of the phenomenology quite well. Our description, however, produces a roughly logarithmic creep function rather than the observed power-law behavior [4,11]. Fluidization at fast inelastic strains [7] has yet to be considered. Active contraction and inelastic deformation at slow rates require a more elaborate approach.

*Discussion.*—Our glutaraldehyde fixation experiments elucidate that stress stiffening in fibroblasts [7] is due to the nonlinear elasticity of the cytoskeleton, and is unrelated to biological signaling or cytoskeletal restructuring. In agreement with our results, very similar stiffening is known from *in vitro* biopolymer networks [18]. To date the precise microscopic mechanism remains unclear; stretching [18,19] and bending [7,20] of single filaments as well as filament alignment [21] have been proposed.

The stiffening elastic elements will dissipate their stored energy upon bond rupture. In loading experiments at relatively fast rates (from Fig. 5), the energy required to reach

the inelastic regime is about 1 $\mu$N $\mu$m $\simeq 2.5 \times 10^8 k_B T$. It has been shown for cells, that dissipation increases by 2 orders of magnitude with respect to bond energies [22]. Considering typical bond energies of about 10 $k_B T$ [23] and 100 nm for the mesh size [1], we estimate that $10^6$ bonds in a 10 $\mu$m cell, roughly 10% of the bonds, must be ruptured before the cell enters the inelastic regime. As a function of the force per bond $f$, dissociation rates are known to increase as $\sim e^{f/f_0}$, where $f_0 \simeq 10$ pN [24,25]. This provides a natural explanation for the logarithmic overstress rate dependence in Fig. 5(b). With an actin mesh size of 100 nm and about $10^4$ load bearing filaments, typical biological adhesion forces of 10 pN result in a drag force $\mathcal{D}$ of about 100 nN, which is indeed the correct order of magnitude. Interestingly, the inelastic stretch rate where the logarithmic trend breaks down [Fig. 5(b)] is of the order of $10^{-3}\mathrm{s}^{-1}$, a typical rate for active cell processes such as crawling and contraction [1,3]. Thus, spontaneous bond dissociation may be what limits active phenomena to long time scales [2].

A living cell must not yield within the physiological ''working range'' of mechanical stress. Kinematic hardening fulfills this requirement and confers stability to the cell; upon a large stretch, weak spots in the cytoskeleton flowing inelastically will increase their rest force $\tilde{\mathcal{F}}$ and eventually stabilize. Rather than break at a given spot, the cell prolongs homogeneously along its length. This homogeneous deformation may be behind the robust linearity of the kinematic hardening response. The exact supramolecular mechanism behind this unusual behavior in a soft system is not known at this point. In cells, kinematic hardening may result from a biochemical coupling between cell length and myosin motor activity. However, the phenomenology is known from passive systems such as composite alloys [15] and granular materials [14]. There, the ''backstress'' (corresponding to our $\tilde{\mathcal{F}}$) is a signature of internal stresses, which increase as the inelastic flow leads to energy storage in the mesostructure.

We have shown that, in uniaxial stretching experiments, cell mechanical properties in the studied range of parameters are reflected well by two simple relations: exponential elasticity and viscoplastic linear kinematic hardening. Given the cytoskeletal complexity, the simplicity of our description is unexpected. A complete picture of passive cell rheology down to molecular details seems in close reach.

We thank P. A. Pullarkat for his invaluable advice, K. Kroy for inspiring discussions and support, and S. Sanderius for his critical reading of the manuscript. This work has been funded by the Universität Bayreuth.

*Present address: E22 Biophysik, Technische Universität München, D-85748 Garching, Germany.
†Present address: Biologische Experimentalphysik, Universität des Saarlandes, D-66041 Saarbrücken, Germany.

[1] D. Bray, *Cell Movements: from Molecules to Motility* (Garland Publishing, Inc., New York, 2001), 2nd ed.
[2] O. Thoumine and A. Ott, J. Cell Sci. **110**, 2109 (1997).
[3] P. A. Pullarkat, P. A. Fernández, and A. Ott, Phys. Rep. **449**, 29 (2007).
[4] B. Fabry, G. N. Maksym, J. P. Butler, M. Glogauer, D. Navajas, and J. J. Fredberg, Phys. Rev. Lett. **87**, 148102 (2001).
[5] N. Wang, J. P. Butler, and D. E. Ingber, Science **260**, 1124 (1993).
[6] N. Wang, I. M. Tolic-Nørrelykke, J. Chen, S. M. Mijailovich, J. P. Butler, J. J. Fredberg, and D. Stamenović, Am. J. Physiol. **282**, C606 (2002).
[7] P. Fernández, P. A. Pullarkat, and A. Ott, Biophys. J. **90**, 3796 (2006).
[8] T. Wakatsuki, M. S. Kolodney, G. I. Zahalak, and E. L. Elson, Biophys. J. **79**, 2353 (2000).
[9] P. Fernández, L. Heymann, A. Ott, N. Aksel, and P. A. Pullarkat, New J. Phys. **9**, 419 (2007).
[10] S. Yang and T. Saif, Exp. Cell Res. **305**, 42 (2005).
[11] N. Desprat, A. Richert, J. Simeon, and A. Asnacios, Biophys. J. **88**, 2224 (2005).
[12] G. J. Todaro and H. Green, J. Cell Biol. **17**, 299 (1963).
[13] W. Prager and H. Geiringer, Ergebnisse der Exakten Naturwissenschaften **13** 310 (1934).
[14] S. Nemat-Nasser, *Plasticity: A Treatise on Finite Deformation of Heterogeneous Inelastic Materials* (Cambridge University Press, Cambridge, England, 2004).
[15] U. F. Kocks, in *Unified Constitutive Equations for Creep and Plasticity*, edited by A. Miller (Elsevier Applied Sci., Essex, 1987), p. 1.
[16] Y. C. Fung, *Biomechanics: Mechanical Properties of Living Tissues* (Springer-Verlag, New York, 1993).
[17] C. T. Mierke, P. Kollmannsberger, D. P. Zitterbart, J. Smith, B. Fabry, and W. H. Goldmann, Biophys. J. **94**, 661 (2008).
[18] C. Storm, J. J. Pastore, F. C. MacKintosh, T. C. Lubensky, and P. A. Janmey, Nature (London) **435**, 191 (2005).
[19] E. Kuhl, K. Garikipati, E. M. Arruda, and K. Grosh, J. Mech. Phys. Solids **53**, 1552 (2005).
[20] A. Kabla and L. Mahadevan, J. R. Soc. Interface **4**, 99 (2007).
[21] P. R. Onck, T. Koeman, T. van Dillen, and E. van der Giessen, Phys. Rev. Lett. **95**, 178102 (2005).
[22] E. Décavé, D. Garrivier, Y. Bréchet, F. Bruckert, and B. Fourcade, Phys. Rev. Lett. **89**, 108101 (2002).
[23] A. Mogilner and G. Oster, Biophys. J. **71**, 3030 (1996).
[24] G. I. Bell, Science **200**, 618 (1978).
[25] D. A. Simson, M. Strigl, M. Hohenadl, and R. Merkel, Phys. Rev. Lett. **83**, 652 (1999).